

Scaling behavior of large scale growth of the microcrystalline silicon films

W. ZHAO^{a,b}, J. CHEN^{a,*}, S. SONG^b, L. XU^b, T. HONG^b, X. ZHANG^b

^a*School of Physics and Telecommunication Engineering, Laboratory of Quantum Information Technology, South China Normal University, Guangzhou, China, 510006, People's Republic of China*

^b*College of Engineering, south china agricultural university, Guangzhou, 510642, People's Republic of China*

An important concern in the deposition of thin microcrystalline silicon ($\mu\text{c-Si}$) films is to obtain the dynamic scaling exponent. We have analyzed the dynamic scaling exponent of $\mu\text{c-Si}$ thin films on different substrates using surface profilometry. The surface roughness of the thin microcrystalline silicon films and the different substrates both are shown and compared. The results reveals that the abnormal dynamic exponent of thin film on the stainless steel substrate account for shadow effect, and the dynamic exponents of thin films on the c-Si substrate and the glass substrate imply the change of growth mechanism with distance from center.

(Received February 4, 2011; accepted March 16, 2011)

Keywords: Microcrystalline Silicon, scaling, Surfaces and interfaces, Growth mechanism

1. Introduction

In the last few years fabrication of large-area microcrystalline silicon solar cell has a major role to play, as it combines availability and environmental sustainability of the main raw materials [1]. Furthermore, typical deposition processes such as plasma enhanced chemical vapor deposition (PECVD) are compatible with mass-production on rigid and on flexible large-area substrates [2][3]. Recently, intense effort has been devoted to the study of the origin of surface roughening during growth regarding various films prepared by various deposition processes including microcrystalline Si ($\mu\text{c-Si}$) [4][5]. Nevertheless, much less effort has been undertaken into studies associated with large-area microcrystalline Si ($\mu\text{c-Si}$) films.

The dynamics scaling of $\mu\text{c-Si}$ thin films has recently attracted considerable interest both from fundamental and applied viewpoints. Many theoretical and experimental studies have been performed to study the dynamics deposition behavior [6][7]. T. Toyama has studied growth-induced roughening of microcrystalline Si ($\mu\text{c-Si}$) surfaces from the viewpoint of self-similar and fractal structures in conjunction with crystallographic preferential orientations of $\mu\text{c-Si}$ films [8]. Huang zhigao has studied the scaling behavior of the anisotropy magnetic films [9]. However, there is much disagreement for the values of the exponents between theory and experiment. Especially, the dynamics scaling of large-area microcrystalline Si has hardly studied.

In this article, large scale vapor-phase growth of the $\mu\text{c-Si}$ films on the different substrate is discussed in terms of the scaling properties of the growth-induced roughness

derived by surface profilometry with the different distance from center.

2. Experimental details

Undoped $\mu\text{c-Si}$ films were prepared by inductively coupled plasma (13.56 MHz) enhanced chemical vapor deposition (ICPECVD) using Ar-diluted SiH_4 on a substrate temperature of 150 °C [10]. Thickness and Surface morphology of samples were investigated by Xp-1 surface profilometry of the Ambios Technology, Inc. The surface profilometry can measure the surface roughness in large scale and give the more credible parameters than AFM [11]. Silane concentration was 4.0–4.5%, the ICP power was 120 W, and deposition pressures was 0.5 Pa. The 6 cm \times 2 cm c-Si, 6 cm \times 2 cm stainless steel and 6cm \times 2 cm Corning 7101 glass substrates were prepared for the deposition of the $\mu\text{c-Si:H}$ thin films. And the deposition time was 1.5 h.

3. Results and discussion

Fig. 1 summarizes dynamic scaling exponents, β , which are derived from $\mu\text{c-Si}$ films deposited on various substrates, as a function of position. From Fig. 1, we can know the dynamic scaling exponents of thin microcrystalline silicon film on stainless steel substrate are approximately 0.8 and the dynamic scaling exponents of those on the glass substrate and c-Si substrate are 0.35–0.55 and increase with distance from the center. In addition, the β exceeds 0.5 on the glass substrate in some positions.

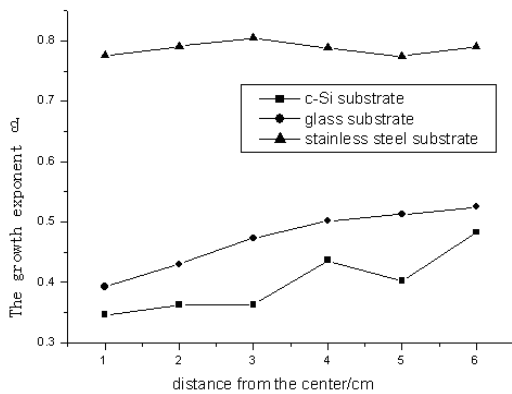


Fig. 1. The growth exponent with distance from the center.

Fig. 2 and Fig. 3 show arithmetic mean roughness and root mean square roughness of $\mu\text{-Si}$ films with distance from the center. The surface roughness of thin microcrystalline silicon film on the stainless steel substrate exhibits large values from two figures. And it random varies with distance from the center due to random varying of surface roughness of stainless steel substrate. The surface roughness of $\mu\text{-Si}$ on the c-Si substrate and the glass substrate slightly increase with distance from the center. And the surface roughness of $\mu\text{-Si}$ on the c-Si substrate is slightly smaller than that of on the glass.

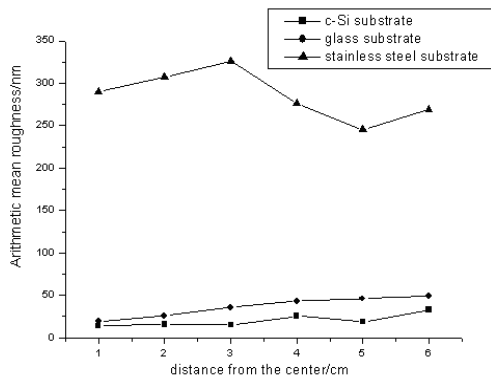


Fig. 2. Arithmetic mean roughness of $\mu\text{-Si}$ film with distance from the center.

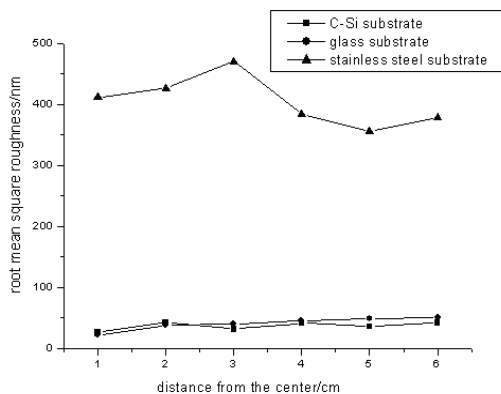


Fig. 3. Root mean square roughness of $\mu\text{-Si}$ film with distance from the center.

Fig. 4 and Fig. 5 show arithmetic mean roughness and root mean square roughness of different substrates with distance from the center. The surface roughness of the stainless steel substrate exhibits large values about several hundreds nanometers from two figures. And it varies irregularly with distance from the center through slapping the surface. What's more, we can find the surface roughness of the thin film on the stainless steel substrate is equal with that of the stainless steel substrate approximately. The surface roughness of the c-Si substrate and the glass substrate is about 10 nanometers.

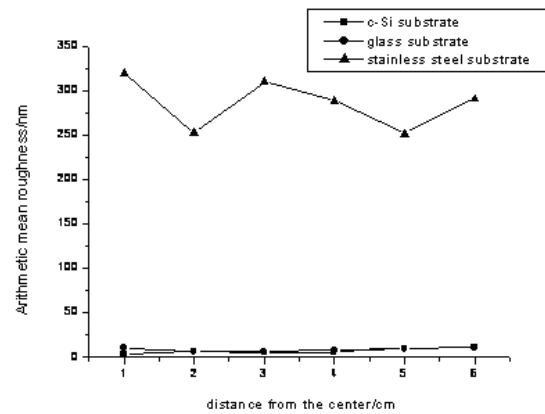


Fig. 4. Arithmetic mean roughness of different substrates with distance from the center.

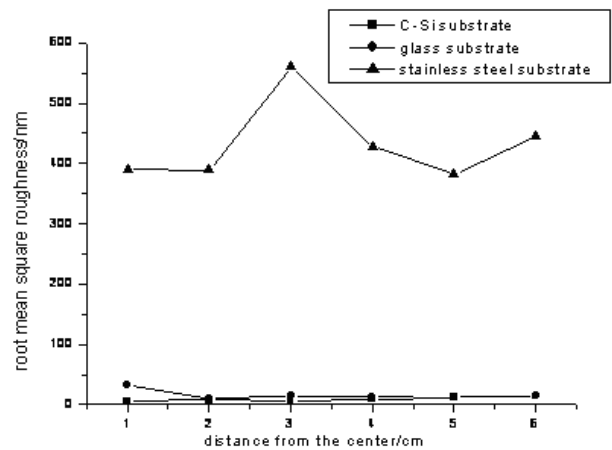


Fig. 5. Root mean square roughness of different substrates with distance from the center.

As shown in Fig. 6 the thickness of $\mu\text{-Si}$ films on different substrates decreases with distance from the center. The change of thickness is slight from 1.9 μm to 1.6 μm on the c-Si substrate, from 1.5 μm to 1.2 μm on the stainless steel substrate. The thin film on the glass substrate exhibits large change from 2.1 μm to 1.4 μm . And the thickness of the thin film on the c-Si substrate is larger than that of on the stainless steel substrate.

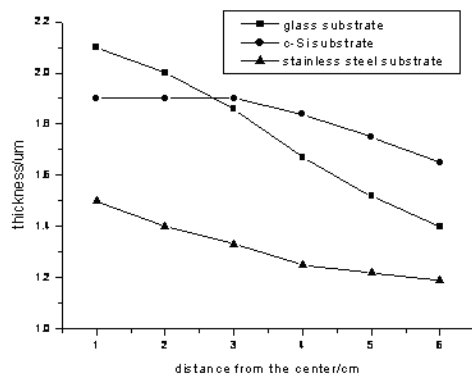


Fig. 6. The thickness of $\mu\text{c-Si}$ films on different substrates with distance from the center.

The thin films are studied by XRD analysis as shown in Fig. 7~9. The XRD spectrums show the thin film on the glass substrate has an amorphous character and the thin film on the c-Si substrate has two orientations. In order to measure the thickness of thin films, we need form the step between the films and substrate. The highest peak on the XRD pattern in Fig. 9 attributes to the c-Si substrate. Due the c-Si substrate has crystalline features, only two orientations in the XRD pattern can be observed in Fig. 9. And the intensity of pattern on the c-Si substrate is about 95, larger than about 65 on the stainless steel substrate.

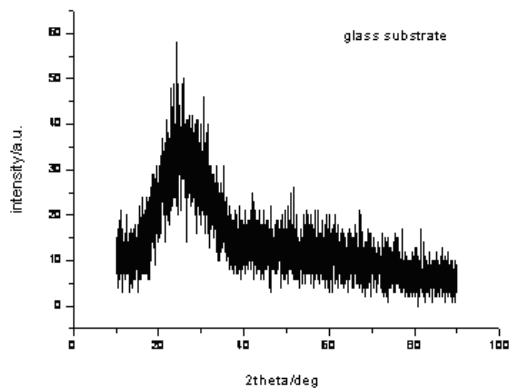


Fig. 7. The XRD pattern of $\mu\text{c-Si:H}$ thin films on glass substrate.

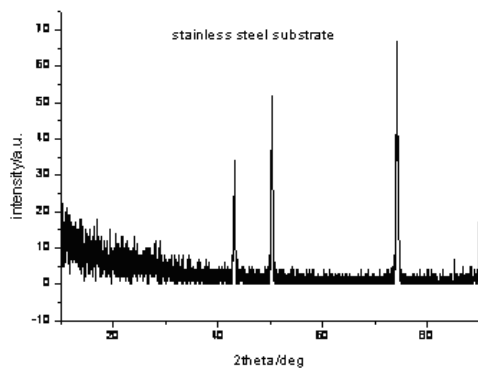


Fig. 8. The XRD pattern of $\mu\text{c-Si:H}$ thin films on stainless steel substrate.

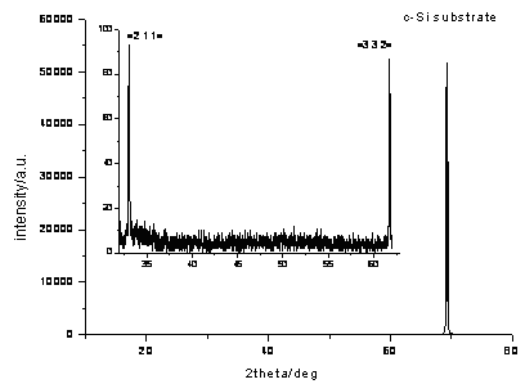


Fig. 9. The XRD pattern of $\mu\text{c-Si:H}$ thin films on c-Si substrate.

The scaling exponents differ in accordance with distance from the center, indicating that the $\mu\text{c-Si}$ surfaces grow with the different vapor-phase-growth mechanisms [12].

During low-temperature preparing thin microcrystalline silicon film growth process, non-thermal equilibrium deposition processes plays an important role. We can infer thin film growth mechanism through research the evolution of thin film surface morphology during the non-equilibrium deposition processes. According to KPZ model [13], film surface roughness, d_s , and film thickness, d , satisfy relationships: $d_s \sim d^\beta$, here β is the dynamic scaling exponent. The different β values correspond to different growth mechanism. When the β is 1/2, the zero diffusion random growth model emerges. Namely reaction precursors do not migrate after random falling on the substrate. When the β is 1/3, finite diffusion growth model has been corresponded. That is to say the reaction precursors have certain migration ability; when β is zero, the infinite diffusion growth model appears. If temperature of substrate is high, reaction precursors have large mobility and move to the most stable thermodynamics position and the film has smooth surface. It is ideal growth mode.

We get dynamic scaling exponent of the thin film on the stainless steel substrate, about 0.8, beyond scale theory in a maximum of 0.5. Abnormal scale behavior of growing films emerges. It indicates that other factors of increasing surface roughness exist in the growth of microcrystalline silicon thin films.

We know forming process of surface roughness of thin films as follows [14]: first, the reaction precursor random falls on the substrate, then diffuses to the nearby position through the surface. The diffusion capacity of adsorbed atom on surface decides the values of β , if the reaction precursor uniform falls on the substrate, maximum value of β is 0.5 [15].

So, if $\beta > 0.5$, it indicates the reaction precursor non-uniform falls on the substrate. Through slapping the stainless steel substrate, the surface roughness has been greatly increased and reaches several hundreds nanometers. Then relationship, $d_s > d^{0.5}$, can be satisfied on the whole growth process on the stainless steel substrate. During the growth of thin films, local high surface can cause shadow effect because the high surface deters part of incoming particles. Shadow effect means high surface adsorbs more

atoms than low surface. MonteCarlo simulation shows that dynamic scaling exponent, β , exceeds 0.5 due to the shadow effect [16]. The large surface roughness on the stainless steel substrate will cause obvious shadow effect, so the β reaches abnormal scale behavior.

On the other hand, due to large local slopes of surface topology appeared, re-emission is believed to occur. So the ions can impact surface many times during the deposition procedure. Because of low ion energy, argon ions and atoms do not damage the surface of films and can only penetrate the subsurface, which would allow ion-induced dehydrogenation to occur at or near the surface [17]. So the three orientations can be observed on the stainless steel substrate in Fig. 8. However re-emission can affect thin film thickness, resulting in decreasing the deposition rate and producing the smallest thin film thickness on the stainless steel substrate in Fig. 6.

Due to crystalline substrate, it is easy to generate crystalline thin film on the c-Si substrate in Fig. 9. And the thin $\mu\text{-Si}$ film on the glass general shows amorphous composition in Fig. 7.

From Fig. 1, we can know the β increases with position on the glass and c-Si substrate, indicating thin film growth model from finite diffusion growth model to zero diffusion random growth model. It proves the diffusion capacity of the reaction precursors on the c-Si and glass substrate become gradually small with distance from center. The temperature is crucial factor for the diffusion capacity. The temperature gradient on the glass substrate and the c-Si substrate results in the gradient of diffusion coefficient from center to edge on the substrates. Similarly the temperature decides thin films deposition rate due to affecting sticking coefficient and evaporation coefficient. The thickness gradients of thin films in Fig.6 are also caused by the temperature gradients on the glass substrate and the c-Si substrate. [18]

What's more, from Fig. 1 we can observe that the diffusion capacity of the reaction precursor on the c-Si substrate is larger than that on the glass substrate. It should be reason that c-Si substrate is smoother than glass substrate which can be express from Fig. 4 and Fig. 5. This point can also be observed in Fig. 2 and Fig. 3 that the surface roughness of thin film on the c-Si substrate is smaller than that of on the glass. The same reason can be explain why in Fig. 6 the thickness gradient on glass substrate is larger than that on the c-Si substrate.

However, the large surface roughness on the stainless steel substrate becomes more crucial than the temperature gradient. So the β keeps basically large value on the stainless steel substrate in Fig. 1 and the film thickness also exhibit small gradient in Fig. 6.

4. Conclusions

In summary, we have analyzed the dynamic scaling exponents of $\mu\text{-Si}$ thin films on different substrates using surface profilometry. The abnormal dynamic scaling exponent of about 0.8 of $\mu\text{-Si}$ thin films on stainless steel substrate indicates the growth mechanism is correlated with the shadowing effect caused by rough surface of substrate. The rough surface on the stainless steel substrate is also main the crucial factor that the thin film exhibits crystalline phase and forms thickness gradient.

The dynamic scaling exponents of $\mu\text{-Si}$ thin films on the c-Si substrate and the glass substrate show the growth mechanism transit from finite diffusion growth model to zero diffusion random growth model. Temperature gradient is main reason which forms the surface roughness and the thickness gradient too. However under this circumstance, the XRD pattern is decided to substrate composition.

Acknowledgments

This work was supported by the Natural Science Foundation of Guangdong Province (10151063101000048) and Special Fund for Agro-scientific Research in the Public Interest of China (No. 200903023).

References

- [1] S. Ferrero, P. Mandracci, G. Cicero, F. Giorgis, C. F. Pirri, G. Barucca, *Thin Solid Films* **383**, 181 (2001).
- [2] J. S. Yoo, G. J. Yu, J. S. Yi, *Solar Energy Materials & Solar Cells* **95**, 2 (2011).
- [3] N. Budini, P. A. Rinaldi, J. A. Schmidt, R. D. Arce, R. H. Buitrago, *Thin Solid Films* **518**, 5349 (2010).
- [4] S. Prakash, M. B. Karacor, S. Banerjee, *Surface Science Reports* **64**, 233 (2009).
- [5] Y. Takeda, S. Yoshimura, M. Takano, H. Asano, M. Matsui, *Journal of applied physics* **101**, 09J514 (2007).
- [6] Z. G. Huang, F. M. Zhang, Z. G. Chen, Y. W. Du, *Eur. Phys. J. B* **44**, 423 (2005).
- [7] M. Acharyya, *Phys. Rev. E* **69**, 027105 (2004).
- [8] T. Toyama, T. Kitagawa, W. Yoshida, Y. Sobajima, H. Okamoto, *Journal of Non-Crystalline Solids* **352**, 941 (2006).
- [9] H. Lai, Z. G. Huang, R. Q. Gai, W. F. Zheng, J. X. Li, C. H. Jia, D. Chen, Y. N. Shen, *Journal of Magnetism and Magnetic Materials* **303**, e406 (2006).
- [10] W. F. Zhao, J. F. Chen, Y. Wang, R. Meng, Y. R. Zhao, S. Y. Shao, J. Y. Li, Y. Zhang, *Chin. J. Chem. Phys.* **23**(4), 447 (2010).
- [11] W. F. Zhao, J. F. Chen, R. Meng, Y. Wang, H. Wang, C. F. Guo, Y. Q. Xue, *Applied Surface Science* **256**, 2009 (2010).
- [12] D. M. Tanenbaum, A. L. Laracuente, A. Gallagher, *Physical Review B* **56**(7), 4243 (1997).
- [13] M. Karder, G. Parisi, Y. C. Zhang, *Phys. Rev. Lett.* **56**, 889 (1986).
- [14] M. S. Valipa, T. Bakos, E. S. Aydil, D. Maroudas, *PRL* **95**, 216102 (2005).
- [15] M. Kondo, T. Ohe, K. Saito, T. Nishimiya, A. Matsuda, *J. Non-Cryst. Solids* **227-230**, 890 (1998).
- [16] J. T. Drotar, Y. P. Zhao, T. M. Lu, G. C. Wang, *Phys. Rev. B* **62**, 2118 (2000).
- [17] J. Robertson, *Mater. Res. Soc. Symp. Proc.* **609**, A.1.4.1. (2000).
- [18] M. S. Valipa, T. Bakos, D. Maroudas, *Physical Review B* **74**, 205324 (2006).

* Corresponding author: chen_junfang@126.com